DOI 10.1007/s11141-015-9621-2
Radiophysics and Quantum Electronics, Vol. 58, No. 7, December, 2015
(Russian Original Vol. 58, No. 7, July, 2015)

FRACTAL MODEL OF A COMPACT INTRACLOUD DISCHARGE. I. FEATURES OF THE STRUCTURE AND EVOLUTION

D. I. Iudin and S. S. Davydenko *

UDC 551.594.2

We propose a new model of a compact intracloud discharge considered as the result of interaction between two (or more) bipolar streamer structures formed in a strong large-scale electric field of a thundercloud. The model assumes two stages of the compact discharge development. At the preliminary stage, two or more bipolar streamer structures appear successively in the thundercloud in the region of a strong electric field (at the boundaries between the regions of the main positive and the main negative electric charges or between the main positive charge region and the top negative screening layer). The time of development of such structures is determined by the characteristics of the conducting channels that form them and can reach tens of milliseconds. Spatiotemporal synchronization of the bipolar streamer structures is provided by the altitude modulation of the electric field, which, in particular, can originate from a large-scale turbulence of the cloud medium or the stream instability. It is shown that a single bipolar streamer structure accumulates significant electric charges of different signs at its ends as it develops. The start of the main stage of a compact intracloud discharge corresponds to the occurrence of the conducting channel (breakdown of the gap) between the mature streamer structures. The electric charge accumulated at the adjacent ends of the structures at this stage is neutralized over a time much shorter than the duration of the preliminary stage. The parameters of the current pulse are in good agreement with the estimates of the current of a compact intracloud discharge which were obtained in the transmission-line approximation.

1. HISTORY OF THE STUDIES AND PHYSICAL MODELS OF COMPACT INTRACLOUD DISCHARGES

The results of observations of unusual intracloud discharges, whose electric field in the far zone had the form of a single bipolar pulse with a duration of 10 to 30 μs and accompanied by a high-power short burst of high-frequency radiation, were first published in [1]. Later, these electric sources were qualified as a separate class and named compact intracloud discharges (CIDs). Despite the multi-year studies of CIDs and the significant volume of experimental data accumulated to date, the nature of this phenomenon is in many respects unclear. In this paper, we propose a new model of compact intracloud discharges, which is based on the fractal approach to the description of their electric structure.

1.1. History of the studies of compact intracloud discharges

The results of detection of electromagnetic radiation of electric cloud discharges with unusual properties were published in the early 80s of the last century [1]. The main feature of such discharges was a high-power burst of high-frequency radiation at frequencies of 3 to 300 MHz, whose level exceeded considerably the values for typical intracloud discharges and cloud-to-ground discharges. Synchronously with the

* davyd@appl.sci-nnov.ru

Institute of Applied Physics of the Russian Academy of Sciences, Nizhny Novgorod, Russia. Translated from Izvestiya Vysshikh Uchebnykh Zavedenii, Radiofizika, Vol. 58, No. 7, pp. 530–551, July 2015. Original article submitted June 30, 2015; accepted July 27, 2015.

burst of high-frequency radiation, non-calibrated ground-based sensors recorded a characteristic variation in the low-frequency electric field in the form of a bipolar pulse with a total duration of 10 to 20 μs (in the experiment [1], the criterion for the start of the electric-field pulse was the exceeding of the radiation intensity of the given, fairly high level at a frequency of 3, 139, or 295 MHz). According to [1], the duration of a bipolar pulse by far exceeded the duration of the high-frequency pulse recorded in the vicinity of the maximum of the electric field pulse, and the amplitude of the bipolar pulse was about 1/3 of the peak value of the electric field for a typical return stroke. In this case, the direction of the electric field in the first half-period of a bipolar pulse was opposite to the direction of the fair-weather field, i. e., the bipolar pulse had an opposite polarity compared with the field bursts for the negative cloud-to-ground discharge.

In subsequent years, the experimental and theoretical study of such discharges has been the subject of a significant number of works which gave a fairly complete picture of electromagnetic radiation. In particular, the authors of [2] performed wide-band measurements of the radiation component of the electric field E and its derivative $\mathrm{d}E/\mathrm{d}t$ for several tens of short bipolar pulses and, using the measurement data on $\mathrm{d}E/\mathrm{d}t$, calculated the spectral densities of the energy and power of the electric-field pulse. By normalization and averaging of the bipolar pulses of the positive polarity (when the electric field on the first half-cycle of the pulse is directed upwards for the ground-based observer), the authors of [2] obtained the following pulse parameters: duration of the initial (positive) part of the pulse at HPPW 2.4 μs, interval between the maxima of the positive and negative field 11 μs, ratio of these maxima 8.9, and total duration 20–30 μs. Average peak value of the electric field of the pulse calculated for a distance of 100 km from the discharge was (8 ± 5.3) V/m (0.72 of the corresponding value for the average pulse of the return-stroke field), and the average peak power of the field derivative was equal to (20 ± 15) V/(m·μs). No variations in the background electric field were observed on a 400 μs interval of measurement, and the profile of the electric-field derivative of the pulse contained a considerable noise component compared with the corresponding profile for other cloud discharges. In [2], short pulses of both polarities were detected (the positive pulses dominated), but no significant dependence of the pulse shape on the pulse polarity was observed. Quantitative analysis of the energy spectrum of the electric field of bipolar pulses has shown that at frequencies of hundreds of kilohertz to 8 MHz this spectrum is comparable with the radiation spectrum of a typical return stroke, but already at a frequency of 18 MHz, at which the radiation spectrum of the return stroke decreases to the noise level, the spectrum of short bipolar pulses exceeds it by 16 dB, extending to above 50 MHz. Thus, in [2] the conclusion in [1] that these discharges are the most powerful source of high-frequency radiation in thunderclouds was confirmed. Wide-band measurements of bipolar pulses of the electric field at frequencies of 3 to 50 MHz were also presented in [3], where it was found that the pulses of the positive and negative polarities have different durations and there is no time correlation of the positive and negative polarity pulses with any known lightning activity in the cloud.

Soon after the above ground-based measurement data were published in [4–6], more than 500 unusual pulse pairs of high-frequency radiation were recorded onboard the ALEXIS satellite. The dispersion of burst pairs, which is well seen in their dynamic spectra, indicated that their source is located under the ionosphere. Therefore, in [4, 5] such bursts were called transionospheric pulse pairs (TIPPs). According to [4, 5], in the range 28–95 MHz the transionospheric pulse pairs are radiation bursts with a duration of 1 to 20 μs (the average duration is 2–4 μs) separated by a time interval of 10 to 100 μs (the average interval is 50 μs). The pulse intensity exceeded by 20–40 dB the background level, and the pulse power in the considered range was at least an order of magnitude greater than the radiated power of a typical lightning discharge. In the range 117–166 MHz, the statistical characteristics of transionospheric pulse pairs differed only slightly in general from their characteristics in the lower part of the very high-frequency range (VHF, from 30 to 300 MHz) except for the decrease in the dispersion and average delay between the pulses, which was 37μs [6]. Both in the low- and high-frequency parts of the VLF range during recording of a pair of pulses (the duration of a record was 7 to 100 ms), the radiation of lightning discharges was not observed as a rule. The authors of [4–6] made two assumptions about the origin of pulse pairs. The first assumption was that the second pulse is the reflection of the radiation of a pulsed high-altitude source from the Earth's surface. The second

assumption is that both pulses are radiated by different, but correlated sources, whose connection is not clear.

The recording of such subionospheric pulse pairs (SIPPs) in the high-frequency range (HF, from 3 to 30 MHz) in the course of ground-based observations has not clarified the origin and the nature of the second pulse [7]. An advantage of ground-based observations was a more exact determination of the position of the source: the radius of the region of its possible location varied from 300 to 520 km as the source altitude varied from 5 to 15 km and was much less than the radius of the ALEXIS surveillance area, which was 3000 km. This has led to the conclusion that about 350 subionospheric pulse pairs of the 500 observed ones corresponded to the regions of close thunderstorm activity, and in other cases the thunderstorm activity was observed at a distance of up to a few thousand kilometers. Moreover, all the subionospheric pulse pairs were recorded in the period of 20:00 to 04:00 LT, which is also indicative of their relation with the regional thunderstorms. The characteristics of subionospheric and transionospheric pulse pairs were similar except for the absence of the dispersion and mode splitting in ground-based observations of almost all of the events. Comparison of the dispersion characteristics of the ionosphere-reflected radiation of a remote lightning discharge and seven recorded subionospheric pulse pairs with dispersion allowed the authors to conclude about the close (no more than a few ten kilometers) location of their sources and the thundercloud. On the whole, according to [7], the recording of subionospheric pulse pairs is evidence for the existence of a separate source of the second pulse since in ground-based observations the presence of the second pulse cannot be explained by the reflection of the initial pulse from the Earth's surface.

Important characteristics of short bipolar pulses were obtained in [8] based on the data of two multipoint systems of recording of the electric field and high-frequency radiation in the range of 3 to 30 MHz. In this case, the features of tuning of the trigger system of sensors provided the recoding of only the positive-polarity pulses. Besides the average (over 24 events) characteristics of short bipolar pulses of the electric field and respective HF radiation bursts for three thunderstorms in New Mexico and Texas (USA; see Table 1), the location of the radiation source was determined for the first time in that paper. The distance to the source was determined by the signal delay time at the spatially separated stations, and the altitude of the source, by the delay of arrival of the signals reflected from the ionosphere and the Earth and ionosphere with respect to the pulse propagating without reflections, by the shortest distance. As a result, it was found that the sources of bipolar pulses are located in thunderclouds at altitudes of 8 to 11 km above sea level, near the regions with a radar-signal reflection level over 40 dBZ. As in the previous studies, the authors of [8] noted no correlation of short bipolar pulses with any known lightning activity in the cloud and reported that bipolar pulses were almost always the only event on the 5 to 50-ms interval. The same is also true for the HF radiation burst.

As a result of comparing the above data on the HF radiation burst that is synchronous with a short bipolar pulse of the electric field and the parameters of transionospheric pulse pairs, the authors of [8] came to the conclusion that the physical phenomenon is the same. The second transionospheric pulse is the reflection of the initial pulse from the Earth's surface, which gives a natural interpretation of the different delays between the pulses in the different frequency ranges [4-6]. The point is that observations of the pulse pairs in the lower part of the VLF range were performed over equatorial regions (see [4, 5]), and in the upper part of the VLF range, over the territory of the USA (see [5]), where the altitude of the thunderclouds is lower than near the equator. If the VLF pulse source is located in the vicinity of the top of a thundercloud, then the delay between the pulses is different in these cases. This assumption also explains the common situation in which the intensity of the second pulse in the pair is higher than that of the first pulse (see [4, 5]), which can be due to the inhomogeneous directivity pattern of the source.

Since short bipolar pulses of the electric field in [8] were recorded exclusively in the far zone, their parameters can conveniently be used for estimation of the characteristics of the corresponding source. According to [8], the average change in the dipolar moment of the bipolar-pulse source was 0.38 C·km with the minimum and maximum values 0.26 and 0.8 C·km, respectively, the average current of the source varied within a few tens to a few hundreds of kiloamperes as the spatial scale of the source varied from 300 to

TABLE 1. Average characteristics of short bipolar pulses of the electric field and synchronous high-frequency radiation bursts in the range 3–30 MHz according to [8].

Characteristics of short bipolar pulses of the electric field	
Field rise time (from 10% to 90% of the maximum), μs	2.3 ± 0.8
Duration of the initial burst of the electric field (at the half-peak level), μs	4.7 ± 1.3
Total pulse duration, μs	25.8 ± 4.9
Peak value of the electric field at the initial (first) burst of a bipolar pulse (at a distance of 100 km from the source), V/m	9.5 ± 3.6
Peak value of the electric field at the second burst of a bipolar pulse (at a distance of 100 km from the source), V/m	-3.9 ± 1.6
Ratio of the peak amplitudes of the electric field at the first and second bursts of a bipolar pulse	2.7
Ratio of the peak amplitudes of the electric field of a bipolar pulse and the pulse due to the return stroke	0.71
Ratio of the peak amplitudes of the electric field of a bipolar pulse and the pulse due to the intracloud discharge	2.6
Characteristics of high-frequency radiation	
Duration, μs	2.8 ± 0.8
Peak value of the field (at a distance of 10 km in the 1-kHz band), mV/m	2.4 ± 1.1
Ratio of the peak amplitudes of the HF field of a compact intracloud discharge and return stroke	9.9
Ratio of the peak amplitude of the HF field of compact and conventional intracloud discharges	29

1000 m, and the pulse propagation velocity of the source current could be close to the speed of light. With allowance for unique features of the radio emission and relatively small sizes of such sources, the authors of [9] suggested to qualify them as a separate class, which was named compact intracloud discharges (CIDs).

The important results concerning the nature of the CIDs were obtained by using LMA (Lightning Mapping Array), a ground-based multipoint system for recording of the VHF radiation of lightning discharges, which is located in New Mexico (USA). The system could not determine the shape and duration of an HF radiation pulse, but located the source to an accuracy of up to a few hundred meters by the delay of the pulse arrival at the measurement points [10]. On the basis of the LMA data, it was found that the positive compact intracloud discharges are located between the regions of the main positive and the main negative charges and, unlike the previous observations, are always connected with the initial breakdown of a conventional intracloud discharge. In this case, most of the intracloud discharges developed without the occurrence of CIDs at the initial stage. According to [10], the sources of high-power VLF radiation of CIDs were distributed in the region with a typical scale of a few hundred meters to one kilometer and, unlike the conventional lightning discharges, were not described by a set of point sources. The estimates [10, 11] have shown that the power of the CID radiation in the range 60–66 MHz could reach 300 kW and is more than an order of magnitude greater than the radiated power of the subsequent intracloud discharge, which does not exceed 10 kW.

The possibilities of recording the radiation of compact intracloud discharges became much wider when the FORTE satellite was launched in 1997 [12]. The satellite receivers recorded radiation at frequencies of 26 to 48 MHz simultaneously for two different polarizations or radiation of one polarization simultaneously in the ranges 26–48 and 118–140 MHz. In addition, high-sensitivity optical sensors were mounted onboard the satellite. The satellite recording of transionospheric pulse pairs in the case where the discharge location is not known made it possible to determine the ratio of altitudes of the sources of different events [12], and the

altitude of the discharge if the data on geographical coordinates of the discharge are available [13], assuming that the second pulse is the reflection of the first pulse from the Earth's surface. Geographic coordinates of the discharge were determined, in particular, from the data of the electric field recording in the VLF/HF range (at frequencies of 3 to 300 kHz) by the multipoint systems LASA (Los Alamos Sferic Array) [14] and NLDN (National Lightning Detection Network) [15].

Analysis of the ground-based and satellite measurement data on the radiation of compact discharges made it possible to determine their location, altitude, and optical brightness. First of all, it was shown, to an accuracy of determining the FORTE location, that the sources of a short bipolar pulse of the electric field and transionospheric pulse pairs coincide in space and in time for the cases of combined recording of the events in the VLF/LF and HF/VHF ranges [16, 17]. It was found that the high-frequency transionospheric pulse pairs with effective power greater than 40 kW in the range 26–48 MHz and duration 3–5 μs are weakly polarized, incoherent, observed separately from other phenomena, or initiate an intracloud discharge, whose radiation in the VHF range is much weaker than the CID radiation [16, 18]. When the CID radiation is recorded simultaneously in the low-frequency (LASA) and high-frequency (FORTE) ranges, it was found that the number of transionospheric pulse pairs exceeds the number of short bipolar electric-field pulses. The CID radiation pulse of a compact discharge, as a rule, is not accompanied by the low-frequency component in the case where the CID initiates an intracloud discharge and the leader development. If the high-frequency pulse is accompanied by the formation of a short bipolar electric-field pulse, then, conversely, the intracloud discharge does not develop [18]. Irrespective of the formation of the bipolar electric-field pulse, compact intracloud discharges radiate rather weakly in the optical range compared with the conventional lightning discharges [19, 20]. Among the recent results concerning the satellite observations of the CID radiation, we mention the paper [21], in which specific differences of the direct and Earth-reflected transionospheric pulses were observed at a frequency of 130 MHz, and the ionospheric effect could be neglected.

The high-frequency CID radiation pattern obtained in the course of space-borne experiments is supplemented in a natural way with the results of recording of the CID radiation by ground-based systems. This is due to the fact that some of the CID characteristics, in particular, the polarity and detailed spatial structure, can be determined only by ground-based recording of the electric field. As the main results of ground-based CID observations obtained in recent years, we mention the following. In [17], based on the analysis of almost 100,000 short bipolar pulses recorded by the LASA system, it was found that compact discharges of different polarity appear at different altitudes. The average height above the Earth's surface for the positive and negative CIDs was 13 km (for the range of discharge heights from 7 to 15 km) and 18 km (for the range of discharge heights from 15 to 20 km), respectively, and the ratio of the numbers of positive and negative discharges was 58:42. The different heights of initiation of the positive- and negative-polarity CIDs correspond to the regions with different direction of the intracloud electric field. Namely, the lower range of heights corresponds to the boundary of the regions of the main negative and the main positive charges, and the upper range, to the boundary of the regions of the main positive charge and the negative screening layer.

The authors of [22] presented the first (and unique for now) estimates of the CID charge moment, which are based on records of the electric field of seven compact discharges in the near zone. According to [22], the charge moment of CIDs lied in an interval of 0.15 to 2 C·km with an average value of about 1 C·km. The authors of [23] analyzed correlation between the rate of occurrence of CIDs and conventional lightning discharges, as well as the rate of convection in the thunderclouds above Great Valleys (USA) from May to July 2005. Comparison of the LASA and NLDN data and the radar sounding results has shown the following. First of all, it was found that the rate of occurrence of CIDs correlates only weakly with the rate of convection in the thundercloud and the rate of occurrence of the conventional lightning discharges. On the one hand, in the clouds with weak convection the compact discharges were not detected, while the clouds with CIDs, on the contrary, always had a deep convection (in particular, for such clouds the region with a radar-signal reflection level of more than 30 dBZ was located 4–5 km higher, and the maximum of the reflection level was 10–13 dB higher than for the conventional lightning discharges. On the other hand, the

CIDs could not appear at all in the thunderstorm cells with the deepest convection. An important feature of compact discharges was their spatiotemporal clustering. Namely, most of the CIDs were recorded in several strong thunderstorms (in particular, 34% of all CIDS were detected at the front of strong thunderstorm cloudiness for 11 h on May 24–25, 2005). It was also found that the number of CIDs does not exceed 0.5% of the total number of lightning discharges. The CIDs of both polarities could be recorded in one cloud, and the number of positive CIDs was about 77% of all recorded compact discharges.

The conclusions on the effect of the rate of convection on the CID development and exceeding of the positive compact discharges, which were obtained in [23], generally conform to the results of measurements in other regions and weather conditions (see, in particular, [14, 24–26]). However, the rate of occurrence of CIDs relative to the total number of lightning discharges changes drastically depending on the geographic latitude of observations in the range from more than 3% in Florida (USA) [14, 24] to 0.034% in North China [25] up to the full absence in Sweden [26]. Analysis of observations of the positive CIDs in Florida (USA) confirmed their predominantly singular nature (about 73% of the events were not related with the conventional lightning discharges). Compact discharge pairs (about 4% of the events), separated by a time interval of 43 to 181 ms [27], were recorded for the first time there. In [28], based on records of 244 short positive bipolar pulses of the electric field it was suggested to categorize them in shape (the "classical" smooth bipolar pulse was observed only in 5% of the cases. It was also noted in [28] that the CIDs are mostly isolated in space and in time with respect to other discharges in the cloud, while the CID altitudes correspond well to the results of [17]. A comparative analysis of the properties of the positive and negative CIDs based on the VLF/LF electric-field measurement data are presented in [29], where, besides the different heights of location of the different-polarity CIDs, it was noted that the negative CIDs, as a rule, do not ensure the greater amplitude of the bipolar pulse of the electric field and are more separated in time. It was also mentioned that, despite the greater number of positive CIDs on the average, the rate of occurrence of the negative compact discharges was higher on some time intervals than that of the positive ones.

1.2. Physical models of compact intracloud discharges

One of the first assumptions on the CID nature was made in [1], where it was suggested that the observed radiation bursts can be interpreted as the consequence of the very fast K process. However, the characteristic times of the electric-field variation in the K processes (about 1 ms) by far exceed the time scales of the CIDs, and these variations usually have the form of a sequence of jumps separated from each other by 10–30 ms [30], in contradiction to the predominantly singular nature of the low-frequency electric-field bursts for CIDs. In addition, the millisecond electric-field discharges that are typical of the K processes are not observed for CIDs, and the power of the VHF radiation exceeds by orders of magnitude the corresponding value for the K processes [31, 32]. In this regard, the interpretation proposed in [1] for CIDs is not satisfactory.

Another model of the compact discharge occurrence is based on the runaway-electron breakdown mechanism [33, 34]. This mechanism relies on the fact that the deceleration force of an electron in the medium is inversely proportional to its energy. Therefore, in the presence of an external electric field that exceeds some threshold value, an energetic seed electron can be constantly accelerated and gain an energy sufficient for the ionization of neutral molecules. As a result, the so-called secondary electrons appear in the medium. Part of them have a high energy and can also become runaway electrons. The resulting avalanche of runaway electrons and a large number of slow secondary electrons can change drastically the conductivity of the medium and lead to an electric breakdown [35]. The source of seed electrons are cosmic rays, whose energy determines in many respects the shape of the formed pulse of the current and the broadband electromagnetic emission of the electron avalanche.

Indeed, it was shown in [36] that within a simplified description of the electron avalanche as of a growing point charge moving vertically at a constant velocity, it is possible to reach a good agreement between the calculation results and the measurements of the ground electric field at different distances from

the discharge. The best coincidence is reached in the case where the source is not one, but a set of electron avalanches arising at one point with given probability in some time interval. However, detailed interpretation of the CID radiation within the runaway-electron breakdown theory encounters certain difficulties. Some of them are discussed in [37], where on the example of three recorded bipolar CID electric-field pulses it was shown that for their generation, the runaway-electron breakdown should have extreme parameters. First of all, the breakdown-initiating particle of cosmic rays should have an energy of about 10^{21} eV, which exceeds the Greisen–Zatsepin–Kuz'min limit [38]. This circumstance decreases abruptly the probability of such a breakdown. Indeed, according to [37], a particle of the corresponding energy enters a cloud with an area of 100 km^2 once per 67 years. Moreover, in the examples considered, according to [37], the conducting channel is from 8 to 13 km long and the discharge current exceeds 500 kA, which by far exceeds the CID parameter estimates obtained in terms of the transmission line model (see, e. g., [39]). The breakdown itself should develop in an intracloud electric field that exceeds severalfold the critical value in a considerable range of altitudes, but this was never observed in the actual thunderclouds. As concerns the interpretation of the high-frequency CID radiation within the framework of the runaway-electron breakdown mechanism, the problems arising in this case are due to a small (submicrosecond) duration and a narrow directivity pattern of the HF radiation burst, as well as an insufficient radiated power in the upper part of the VLF range [40]. The electron avalanche which provides an acceptable level of high-frequency radiation within the model [40] forms a bipolar electric-field pulse which does not conform to the observations. The narrow beam of the runaway-electron breakdown radiation does not permit one to explain the satellite observations of the transionospheric pulse pairs, and the assumption proposed in [41] about the initiation of two breakdowns by one energetic particle at different altitudes (above the thundercloud and in the mesosphere) was not confirmed experimentally. We also note that the estimates presented in [42] concerning the increase in conductivity of the intracloud medium due to the generation of secondary electrons bring into a question the very mechanism of the runaway-electron breakdown.

Another mechanism of the formation of short bipolar electric-field pulses arising in CIDs has recently been proposed in [43]. According to [43], these bursts are formed with an abrupt lengthening (a jump) of the existing negative leader in a strong electric field of the thundercloud. The radiation source is the currents appearing when the electric charge flows along a well-conducting leader channel in the vicinity of the new-element addition point. Despite the detailed analysis of the dynamics of charges and currents in the leader jump and good agreement between the model data and the far-field observation results (note that this agreement is reached for a fairly long jump of more than 600 m), the approach proposed in [43] does not give an answer to some important questions. Such questions are first of all about the mechanism of the formation of the initial leader channel, which requires weak electromagnetic radiation both in the VLF/LF and HF/VHF ranges and a mechanism for generation of a short high-power burst of HF/VHF radiation in the leader jump. In this meaning, the approach proposed in [43] seems close to the models based on the CID description within the transmission-line approximation, which will be considered in the second part of the work.

On the basis of what was said above, it can be concluded that a self-consistent physical model of compact intracloud discharges is absent at present. In this paper, we propose a new mechanism of the CID initiation, which is based on the fractal approach to describing intracloud electric discharges. A compact intracloud discharge is considered as the result of interaction of two streamer bipolar structures developing in a large-scale nonuniform external electric field. In the first part of this work we consider the features of emergence and evolution of CIDs. In the second part, we discuss the CID radiation in different frequency ranges in terms of the model proposed.

2. THE MODEL OF A COMPACT INTRACLOUD DISCHARGE

The modeling of CIDs is closely related to one of the basic features of the electric discharge in thunderclouds, namely, a combination of the low static conductivity of the intracloud medium and the observed rapid (from a few tens of microseconds in the case of a CID to hundreds of milliseconds in the conventional

lightning discharges) collection of the electric charge from a considerable part of the thundercloud into the discharge channel. The authors of [44–47] proposed a charge collection mechanism based on the formation of a system of conducting channels in the cloud, which actually play the role of an electric drain system. Generally speaking, such a system of conductors should include elements with sizes ranging from the distances between charged particles to the thundercloud scale, which makes its full description extremely difficult. In this regard, all the existing models in some way or other limit the level of spatial details in the discharge description, generally omitting the microphysical processes and small-scale phenomena. In all of the above papers, their authors considered as the conducting element the part of the leader discharge whose development was described within the three-dimensional Poisson equation with allowance for the external electric field and the stochastic model of dielectric breakdown, which was proposed back in [44, 48, 49]. With the algorithms being somewhat different in details, all these models have two significant constraints. Firstly, they do not admit the simultaneous growth of different branches of the discharge and, secondly, the temporal scale is absent in them, resulting in that the discharge branches do not carry currents. The first of these constraints was overcome in [50], where a percolation model of the lightning discharge based on a network of cellular automata was proposed within the self-organized criticality paradigm. Then the currents of the discharge tree were taken into account within the same approach [51, 52], which made it possible to calculate the characteristics of the high-frequency radiation of the lightning discharge. In the present paper, we also use the approaches based on the cellular automata model to describe a compact intracloud discharge. As the element (cell) of the model, we consider the cubic volume of the cloud medium, which may contain some total electric charge. The size of an elementary cell by far exceeds the distance between the physical charge carriers, that is, the cloud particles whose charging can be provided by various electrization mechanisms [53] and some types of instabilities [54, 55] in the thundercloud. Electric (conducting) links between the neighboring elements are stipulated by the initiation of an electric discharge between them, with the electric charge flowing along the conducting channel of the latter. In the macroscopic modeling, it is assumed that only part of the elementary-cell volume is involved in the charge transfer. This is due to the assumption that small-scale, relatively well conducting links within each cell (e. g., streamer structures) encompass only part of the carriers. Otherwise, the whole thundercloud would be permeated with conducting links, which could have changed drastically the development of the electric discharges in them.

We now consider the fundamental differences of the considered model from the previous ones. The first difference concerns the discharge morphology. As was mentioned above, a short, strong burst of CID radiation does not conform to the parameters of a conventional intracloud discharge, which lasts much longer and whose emission is much weaker both in the low- and high-frequency ranges. Within the known mechanisms we cannot explain why the source current strength required for such a radiation is comparable with the return-stroke current in the cloud-to-ground discharge (see, e. g., [39]). In this regard, we assume that a compact intracloud discharge includes two stages, preliminary and main. At the preliminary stage, two bipolar discharges, similar in shape to intracloud discharges, develop at a relatively short distance from each other along the external electric field. Each discharge exists much longer than the CID radiation burst, and over the time of its existence it accumulates a significant charge of different polarity at its opposite ends (in the crown and the root of the discharge). The second, main stage of the discharge starts when the oppositely charged crowns of these discharges come into electric contact as they grow. There appears a current channel connecting the regions with opposite sign of the charge, resulting in that the charge accumulated at the preliminary stage drains along the arising conducting channel in a short time. The second feature of the proposed model is due to the necessity of providing a very low level of electromagnetic radiation both in the VLF/LF and HF/VHF ranges at the preliminary stage of the CID. To this end, we assume that at the preliminary stage, the electric coupling between the elementary cells is a discharge of the streamer type, with relatively weak and mainly slowly varying currents corresponding to weak electromagnetic radiation (the CID radiation will be discussed in more detail in the second part of the work). Note that at the altitudes of the CID occurrence, the length, velocity, and currents of the streamer discharges can widely range in the regions of a strong electric field [56, 57].

Consider in more detail the CID electrodynamics within the framework of the proposed approach.

3. DESCRIPTION OF A SINGLE BIPOLAR STREAMER DISCHARGE

Consider first the dynamics of a single bipolar streamer discharge in a $500 \times 500 \times 500$ m region located in the vicinity of the local maximum of an intracloud electric field. For definiteness, we consider the processes near the boundary between the main positive and the upper (negative) screening layers of the space charge, where, according to observations, the negative CIDs appear. In this case, we neglect the difference in the dynamics and properties of the positive and negative streamers, assuming that their velocities are identical and equal to $5 \cdot 10^5$ m/s [56]. The size of an elementary cell will be assumed equal to $10 \times 10 \times 10$ m, the length of the conducting link between the neighboring cells is of the order of 10 m. This value, generally speaking, is fairly large for the length of a single streamer even with allowance for the pressure drop at the altitudes considered. However, it can be supposed that the electric coupling between the cells is realized either through a set of streamers or a weak-current structure, similar to the recently discovered stalkers [58]. In addition, the characteristics of the electric coupling can develop as a result of multiple passage of the streamer discharge over the same volume. The model time step of the system is equal to $\tau = 20$ μs and is determined by the time of creation of the conducting link between the neighboring cells, i. e., the ratio between the cell size $a = 10$ m and the streamer velocity.

Each ith elementary cell in the simulation domain is put into correspondence with the electric charge q_i accumulated in it. The charge distribution in the cells at the initial time $t = 0$ is given by the distribution of the intracloud electric field $\mathbf{E}(\mathbf{r}, t = 0)$, which will be assumed vertical. Since the considered region is small compared with the sizes of the thundercloud, the initial distribution of the field can be assumed one-dimensional: $\mathbf{E}(\mathbf{r}, t = 0) = \mathbf{z}_0 E_0(z)$, where $\mathbf{z}_0$ is the unit vector of the vertical axis z. In this case, the initial distribution of the charge density in the cloud depends on the vertical coordinate: $\rho(z, t = 0) = \varepsilon_0 \, \partial E_0(z, t)/\partial z$, where ε_0 is the electric constant and the charge in the ith elementary cell, centered at the point with the coordinate $\mathbf{r}_i = (\mathbf{r}_{\perp i}, z_i)$, is equal to $q_i = a^3 \rho(z_i, t = 0)$. To estimate the initial profile of the field at the boundary of the main positive and the upper screening layers, one can use the balloon sounding data on the thunderclouds. These data suggest that in the vicinity of the screening layer ranging from a few hundred meters to more than one kilometer in thickness and located at altitudes of 8 to 15 km above sea level, the electric field strength can reach 50 kV/m [59, 60]. Without going into details of the screening layer formation (see, e. g., [61, 62]), we assume for calculations that the electric field between the main positive and the upper screening layers is the maximum at an altitude of 12 km and reaches 30 kV/m; the region of a strong electric field is about 500 m thick.

The electric charge dynamics in each cell is determined by the presence and state of the electric coupling with the neighboring cells.[1] We assume that the probability of occurrence of the streamer discharge (breakdown) between the neighboring ith and the jth cells depends on the difference of their potentials and is described by the Weibull distribution:

$$P_{ij} = \begin{cases} 1 - \exp\left(- \left| \dfrac{E_{ij} - E_\mathrm{i}}{E_\mathrm{s} - E_\mathrm{i}} \right|^m \right), & E_{ij} \geq E_\mathrm{i}; \\ 0, & E_{ij} < E_\mathrm{i}. \end{cases} \tag{1}$$

Here, m is the Weibull index, $E_{ij} = |\varphi_i - \varphi_j|/L_{ij}$, φ_i and φ_j are the electric potentials of the ith and the jth cells, respectively, L_{ij} is the distance between the ith and the jth cells, and E_s and E_i are the critical and the streamer initiation fields, respectively, such that $E_\mathrm{s} \gg E_\mathrm{i}$. Note that under conditions of laboratory gaps (tens of meters long), the field is of the order of 100 kV/m [56] and can be much lower under conditions of cloud discharges [63]. The physical reason for the local (small-scale compared with the

[1] Note that the characteristic time of development of a streamer discharge is much shorter than the relaxation time of the electric charge due to the finite conductivity of the intracloud medium; therefore, the leak currents can be neglected in this case.

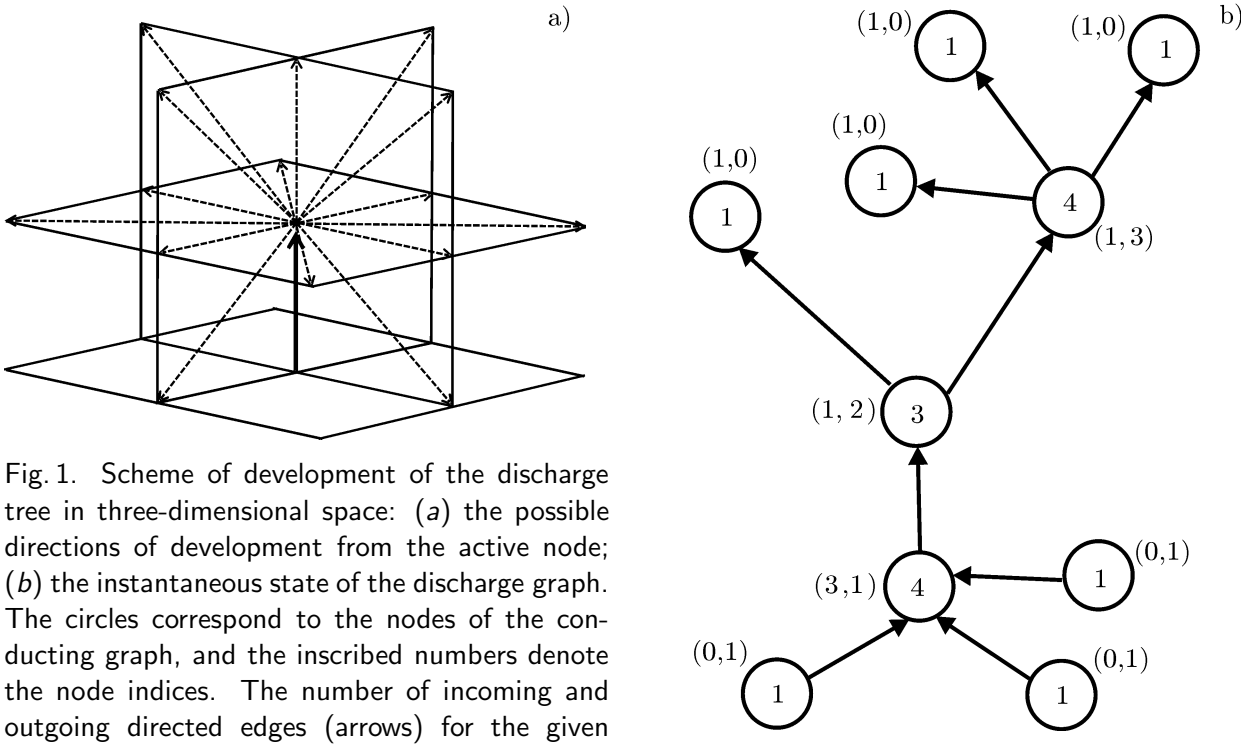

Fig. 1. Scheme of development of the discharge tree in three-dimensional space: (*a*) the possible directions of development from the active node; (*b*) the instantaneous state of the discharge graph. The circles correspond to the nodes of the conducting graph, and the inscribed numbers denote the node indices. The number of incoming and outgoing directed edges (arrows) for the given node is shown in the parentheses.

cell size) enhancement of the field and, correspondingly, the decrease in the fields $E_{\rm s}$ and $E_{\rm i}$ on the cell scale compared with the laboratory values can be natural small-scale irregularities of the charge density [64].

The charge initiation starts spontaneously for two neighboring cells, the probability of a breakdown between which reaches the maximum. As the discharge develops in different parts of the generated conducting structure, new conducting links can be formed, whose probability is described by Eq. (1). The structure of the generated discharge is a directed graph, whose nodes and edges correspond to the cells of the simulation domain and the conducting electric coupling. All nodes of the graph (discharge tree) can be divided into three nonintersecting groups: 1) peripheral nodes that form the outer boundary of the tree, 2) intermediate nodes that successively connect the adjacent links of individual branches, and 3) branch connections, or branching points, that is, nodes that are common for three or more links. If the electric field strength between the peripheral node and the nearest cells exceeds the initiation field, then one or several new conducting links, and the same number of new peripheral nodes, arise with probability (1). If the peripheral node did not activate the links with the neighboring cells, then it dies together with the conducting link that corresponds to it.

To describe the conducting structure, it is convenient to introduce the notion of the node index, which is equal to the total number of incoming and outgoing directed edges (shown by arrows in Fig. 1; the direction of the arrows corresponds to the current direction). For example, the index of a peripheral node is equal to unity, the index of an intermediate node is equal to two, etc. Each of the ith node will be put into correspondence with a pair of numbers (a_i, b_i), which are equal to the number of incoming and outgoing edges, respectively. The quantity $a_i + b_i$ obviously coincides with the node index. The charge initiation corresponds to the occurrence of a pair of adjacent nodes, one of which belongs to the type (1, 0) and another, to the type $(0, 1)$. At the next step of the model time, the state of the active peripheral node of the type (1, 0) converts into the state $(1, n)$, where n is the number of newly activated neighbors of the node considered. Similarly, the state of the active peripheral node of the type (0, 1) converts into the state $(n, 1)$. Thus, the whole set of nodes of the evolving structure is distributed between the types $(1, n)$ and $(n, 1)$ with integer non-negative n. The trunk of the discharge tree is the non-branched core of the structure, which is an oriented chain composed of type (1, 1) nodes and edges that connect them. The trunk ends

with a pair of nodes, one of which belongs to the type $(1, n)$ and another, to the type $(n, 1)$. The type $(1, n)$ nodes with $n \geq 2$ and the connecting edges form the crown, while the type $(n, 1)$ nodes and the connecting edges form the root of the oriented tree (see Fig. 1*b*).

An important feature of the considered model is the presence of a current system that develops in the conducting streamer structure. This makes the discussed model fundamentally different from the previous fractal models based on the assumption of an exponential discharge tree at each step of the model time. In the conducting channels of the discharge tree, there is an electric current, which, on the one hand, makes the potentials at the nodes of the conducting graph equal and, on the other hand, satisfies the continuity law. At each step of the model time, the electric-charge variation in the ith elementary cell is given by the relationship

$$\mathrm{d}q_i = \tau \sum_{j=1}^{a_i+b_i} I_{ij}, \tag{2}$$

where I_{ij} is the electric current between the ith and the jth nodes with conducting link, which is determined by the difference of the node potentials $\varphi_i - \varphi_j$, linear resistance of the link $\Re_{ij}$, and its length L_{ij}, which, depending on the orientation, can take the values a or $\sqrt{2}a$:

$$I_{ij} = \frac{\varphi_i - \varphi_j}{\Re_{ij} L_{ij}}. \tag{3}$$

The electric potential of the ith cell at each step of the model time is determined by its own charge q_i and effective capacitance, which for simplicity is assumed equal to the capacitance of a conducting sphere of radius $a/2$, as well as the total potential of the electric field, which is external with respect to the simulation domain, and other charged cells of the system. The linear-resistance variation is determined by the balance between release and spread of the Joule heat in the discharge channel. Since a detailed description of the dependence of the streamer-channel resistance on the current does not exist, we assume that when a channel appears, its linear resistance is equal to $\Re_0 = 0.1$ MΩ/m, and as the current rises in the channel, its value falls to 1 μΩ/m for currents greater than 1 A. It is assumed that as the current is varied in the channel, a new value of the linear resistance is set immediately. The arising system of conducting channels plays the role of a drain system of the electric charge. Due to the summation of currents of individual channels at the branching points, the current in the trunk of a discharge tree significantly exceeds the currents in its periphery. Note that when moving from the peripheral elements to the trunk, not only the current strength, but also the time of existence of the link increase.

Figure 2 shows an example of the development of a single streamer discharge in the vicinity of the maximum electric field corresponding to the boundary between the main positive and negative screening layers of the space charge (the basic parameters of the model distribution of the field were discussed previously). It is well seen that with the development of a discharge, the profile of the potential between its crown and root becomes flatter; correspondingly, the electric field inside the discharge decreases. The regions of the maximum charge density inside the discharge are concentrated in the crown and root of the discharge at some distance from the peripheral tops, which is due to the finite conductivity of the streamer channels. Thus, a single bipolar streamer discharge as it develops is able to accumulate a significant electric charge and actually forms a distributed dynamic dipole, which plays an important role in the CID development. Note that compared with the duration of the main stage of the CID, the charge in a single bipolar streamer discharge is slowly accumulated (for up to a few tens of milliseconds). The currents in the discharge trunk do not exceed a few amperes, which implies that their electromagnetic radiation is fairly weak.

3.1. The streamer discharge synchronization and the CID initiation

As was mentioned above, the considered model of the CID initiation assumes the formation of two developed bipolar streamer structures which accumulated a significant electric charge before the interaction

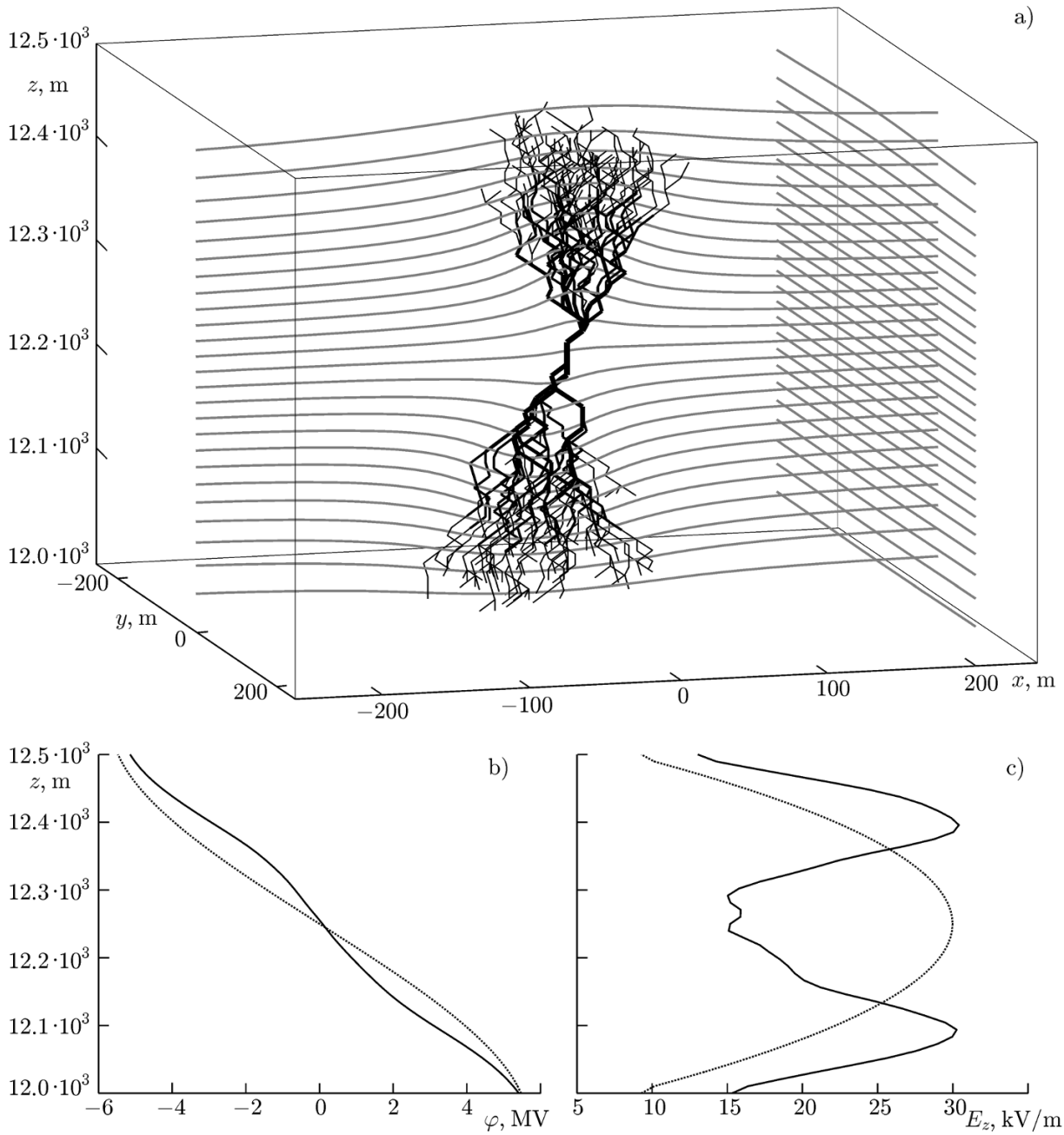

Fig. 2. (*a*) A snapshot of a three-dimensional bipolar streamer discharge in a weakly nonuniform electric channel. The thickness of the graph element corresponds to the current strength in the corresponding conducting channel. Gray lines correspond to the equipotentials in the $y = 0$ and $x = 200$ m planes; hereafter, x and y are the axes of the Cartesian coordinate system, and $\mathbf{r}_\perp = (x, y)$. Altitude profiles of the electric potential (*b*) and the vertical component of the electric field (*c*) before the channel generation (dashed line) and at the stage of a developed discharge (solid line).

time. In this case, spatiotemporal synchronization of the streamer discharges is important: they should develop at the same time at a relatively short distance from each other along the external electric field. It is seen in Fig. 2*b* that, in principle, as a single discharge develops, the electric field at its axis is enhanced at the discharge boundary. Due to this, the field at the discharge axis, especially in the presence of a random small-scale inhomogeneity of the charge density, can exceed at some time the initiation threshold, resulting in one more streamer discharge. However, this method of the discharge synchronization has a

significant drawback: the distance between two discharges is too small for their independent development and for collection of a sufficient space charge before the electric contact. As a result, the field in the gap between the discharges reaches rapidly a breakdown value, and the second discharge becomes part of the more developed first discharge without the CID initiation. Generally, in the presence of the charge density variations with a characteristic scale of the order of the longitudinal (along the external electric field) size of the bipolar streamer structure, the field can exceed the threshold value and initiate the second discharge at much longer distances from the first discharge. As a result, before the contact with the first streamer discharge, the second discharge has time to accumulate an electric charge sufficient for the CID initiation.

The source of large-scale variations of the charge density and, correspondingly, electric field can be the turbulent component of the convective flow, which is enhanced at the upper boundary of the cloud. However, due to the different scales of the charge-density perturbations, a significant spread of the CID parameters should be expected, which, however, is poorly confirmed by the observations. In this regard, it is interesting to study the mechanisms capable of forming a quasiregular large-scale perturbation of the electric field (charge density), against the background of which streamer discharges can develop at the preliminary stage of the CID. A possible mechanism for the formation of the inhomogeneous distribution of the charge density with the necessary spatial scale can be the stream instability, which was first described in [54]. This instability develops in a multicomponent intracloud medium in the presence of a weakly conducting air flow with respect to the heavier intracloud particles. As a result, an exponentially increasing space-charge wave is formed in the cloud; it moves with the convective flow towards the cloud top. The charge-density growth rate in the stream reference frame,

$$\gamma_{\max} = \begin{cases} 4\pi\sigma\,(\Omega/\nu - 1)^2, & \Omega/\nu < 2; \\ 2\pi\sigma\Omega/\nu, & \Omega/\nu > 2, \end{cases}$$

is determined by the plasma-frequency analog for heavy particles, $\Omega^2 = 4\pi Q^2 N/M$, where Q, M, and N are the charge, mass, and density of heavy particles, respectively, the effective frequency ν of their collisions, and air-stream conductivity σ. In this case, the spatial scale $2\pi/k_{\text{opt}}$ of the generated inhomogeneity of the charge density also depends on the air-stream velocity u:

$$k_{\text{opt}} = \begin{cases} \dfrac{\nu}{u}\left(\dfrac{\Omega}{\nu} - 1\right)^{1/2}, & \Omega/\nu < 2; \\ \Omega/u, & \Omega/\nu > 2, \end{cases}$$

According to the estimates [54], the characteristic time of the instability development is of the order of 100 s and the spatial scale of the space-charge inhomogeneity can vary widely from tens to hundreds of meters. Due to the small size of the considered region, the effect of the boundary conditions on the charge density distribution can be neglected. A more detailed analysis of the stream instability with allowance for the charging mechanisms and cloud-particle parameters is presented in [55]. We only note that the mentioned mechanism of the electric-field non-uniformity formation is fairly robust with respect to the characteristics of heavy particles and the strength of the external electric field. The appearance of relatively heavy particles in the upper layers of the cloud can be due to a short-time enhancement of the upgoing streams in the thundercloud. That the local convective flows have a significant effect on the CID initiation is favored by the observed spatiotemporal clustering of compact discharges, which manifests itself as an abrupt rise in the rate of their occurrence in the limited region of a cloud at the boundary of charged layers. According to [23], the rate of occurrence of negative CIDs, which are rarer in general, can exceed for some time the rate of occurrence of positive CIDs. This can be related to the formation of favorable conditions for the synchronous development of streamer discharges due to the stream instability.

Development of the CID in a medium with nonuniform distribution of the electric field and space charge is illustrated in Fig. 3, where the initial large-scale distribution of the charge density in the CID initiation region, which corresponds to the electric-field profile in Fig. 1*c*, is supplemented with a harmonic

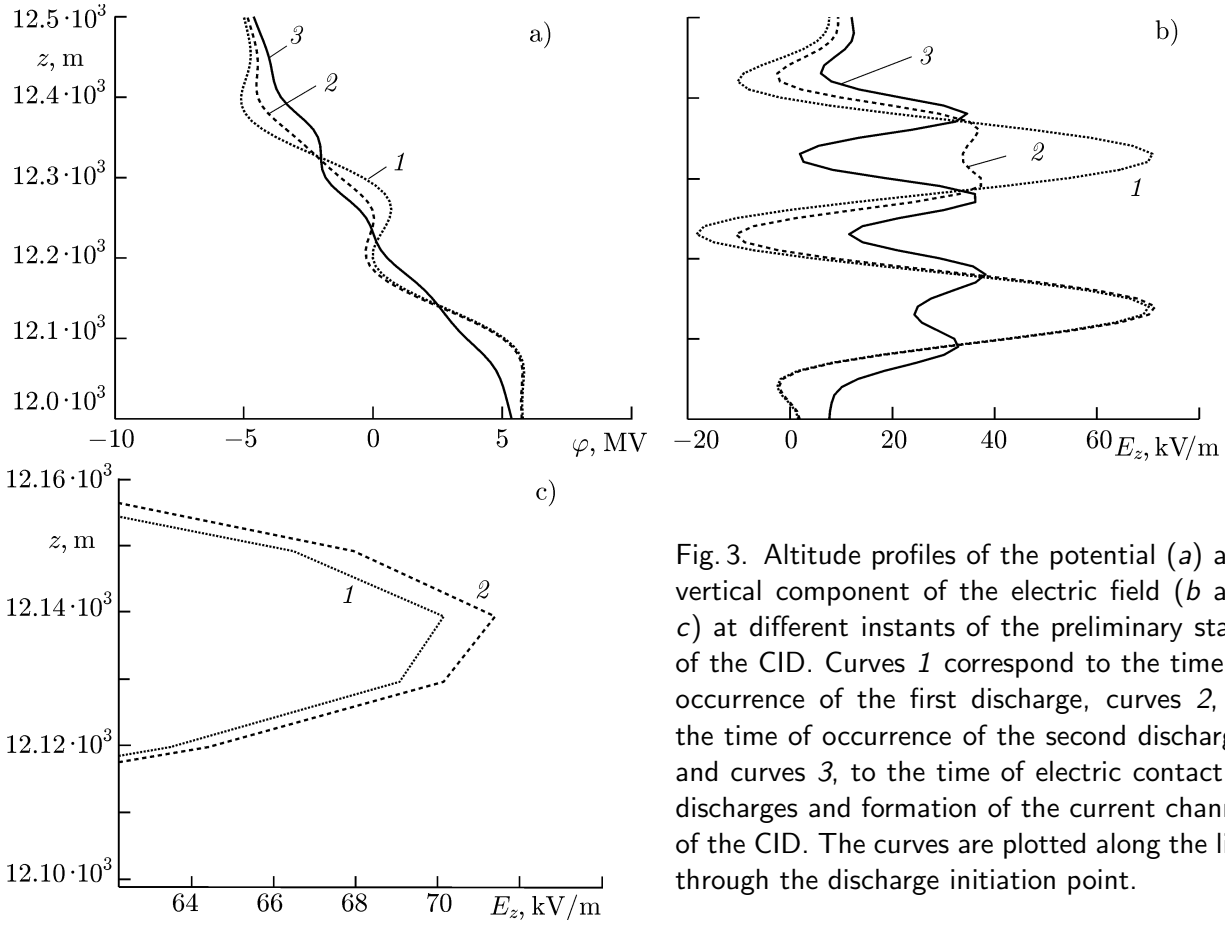

Fig. 3. Altitude profiles of the potential (*a*) and vertical component of the electric field (*b* and *c*) at different instants of the preliminary stage of the CID. Curves *1* correspond to the time of occurrence of the first discharge, curves *2*, to the time of occurrence of the second discharge, and curves *3*, to the time of electric contact of discharges and formation of the current channel of the CID. The curves are plotted along the line through the discharge initiation point.

perturbation with a spatial scale of 200 m (curves *1* in Fig. 3). It is seen that with the development of the first discharge that occurred at an altitude of about 12350 m, the electric field in it increases. Above and below the first discharge, at the altitudes of the perturbation half-period of the negative-polarity field, the total field remains much lower than the initiation field of the streamer discharge. As a result, some sort of a forbidden band for the second-discharge initiation is formed in the immediate vicinity of the first discharge. Conversely, in the neighboring half-periods of the positive perturbation of the field, as the first discharge develops, the conditions of the second-discharge initiation become more and more favorable (in particular, a slight increase in the local field maximum at an altitude of about 12140 m is seen in Fig. 3*c*). As a result, in a medium with the considered quasiperiodic distribution of the charge density, the development of a bipolar streamer discharge leads necessarily to the initiation of the second streamer discharge, which is separated from the first discharge by the region of low electric field. The delay of the second discharge is small compared with the duration of the preliminary stage of the CID and does not lead to a significant difference of the streamer discharges at the time of their electric contact. Note that during the formation of several periods of the spatial inhomogeneity of the charge density there is a possibility for the successive initiation of several CIDs.

Figure 4 shows snapshots of different stages of the CID evolution in a medium with spatially nonuniform electric field, whose distribution at the axis of the calculation region is similar to the profile presented in Fig. 3. It is seen that the second discharge arises with an about 5 ms delay after the first-discharge initiation (see Figs. 4*a* and 4b), and after that both discharges exist simultaneously for a long time (see Fig. 4*c*). As a result of the charge redistribution by each of the streamer discharges, the electric-field drop between the discharges decreases until an electric contact between the streamer structures occurs in about 11 ms after the second-discharge initiation (see Fig. 4*d*).

The description of the main stage of the CID, at which a high-power current channel is formed

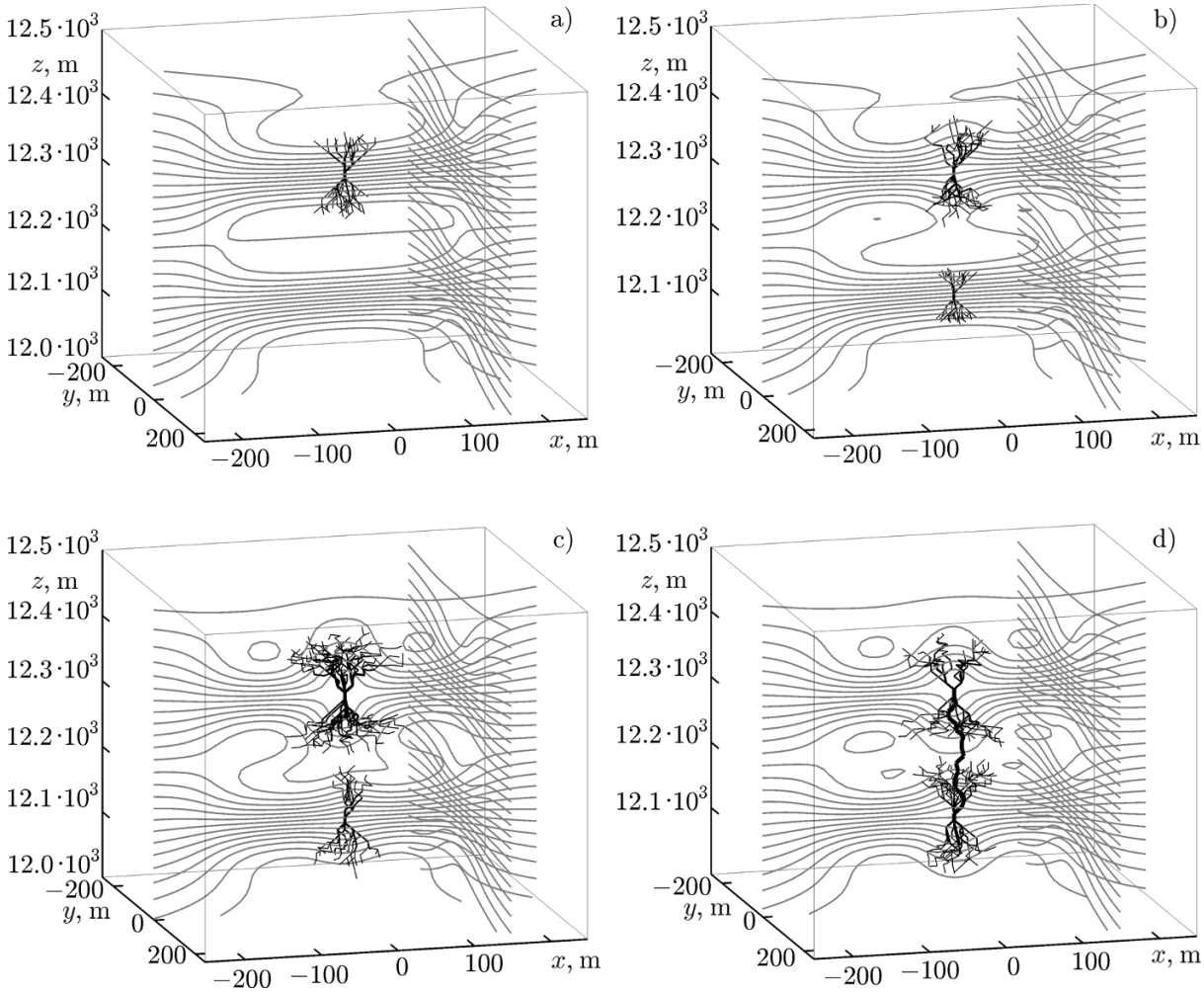

Fig. 4. Successive stages of the CID development in a medium with spatially nonuniform external magnetic field: (*a*) the development of the first streamer discharge in seven steps of the model time ($t = 140$ μs); (*b*) the start of the second-discharge development ($t = 5.06$ ms); (*c*) the simultaneous development of the discharge pair ($t = 7.50$ ms); (*d*) the instant of the electric contact of discharges after 556 steps of the model time ($t = 11.12$ ms) with the formation of a high-current channel. Gray lines correspond to the equipotentials in the $y = 0$ and $x = 200$ m planes.

between the streamer discharges, is closely related to the burst of low- and high-frequency radiation of the CID. The features of the compact-discharge radiation are considered in more detail in the second part of the work. Here, we give only some of the characteristics of the arising burst of current. As was mentioned above, a prerequisite for the formation of a high-power short pulse of current in the CID is the presence of relatively close regions of the space charge with opposite sign, which are formed at the preliminary stage of a discharge. The structure of such regions is illustrated in Fig. 5 showing the initial distribution of the charge density in the cloud and a similar distribution before the breakdown, at the start of the main stage of the CID. It is seen that at this instant the volume charge in the adjacent regions of bipolar streamer discharges is compactly concentrated in the vicinity of the breakdown channel, the charge density before the breakdown being almost twenty times greater than the initial value.

Distribution of the charge density along the conducting channel between the streamer discharges at the time of its occurrence is shown in Fig. 6*a*, and the corresponding distribution of the discharge current at different moments of time after the start of the main stage of the CID is given in Fig. 6*b*, assuming that the velocity of the ionization-wave front is $6 \cdot 10^7$ m/s. It is seen that the amplitude of the discharge

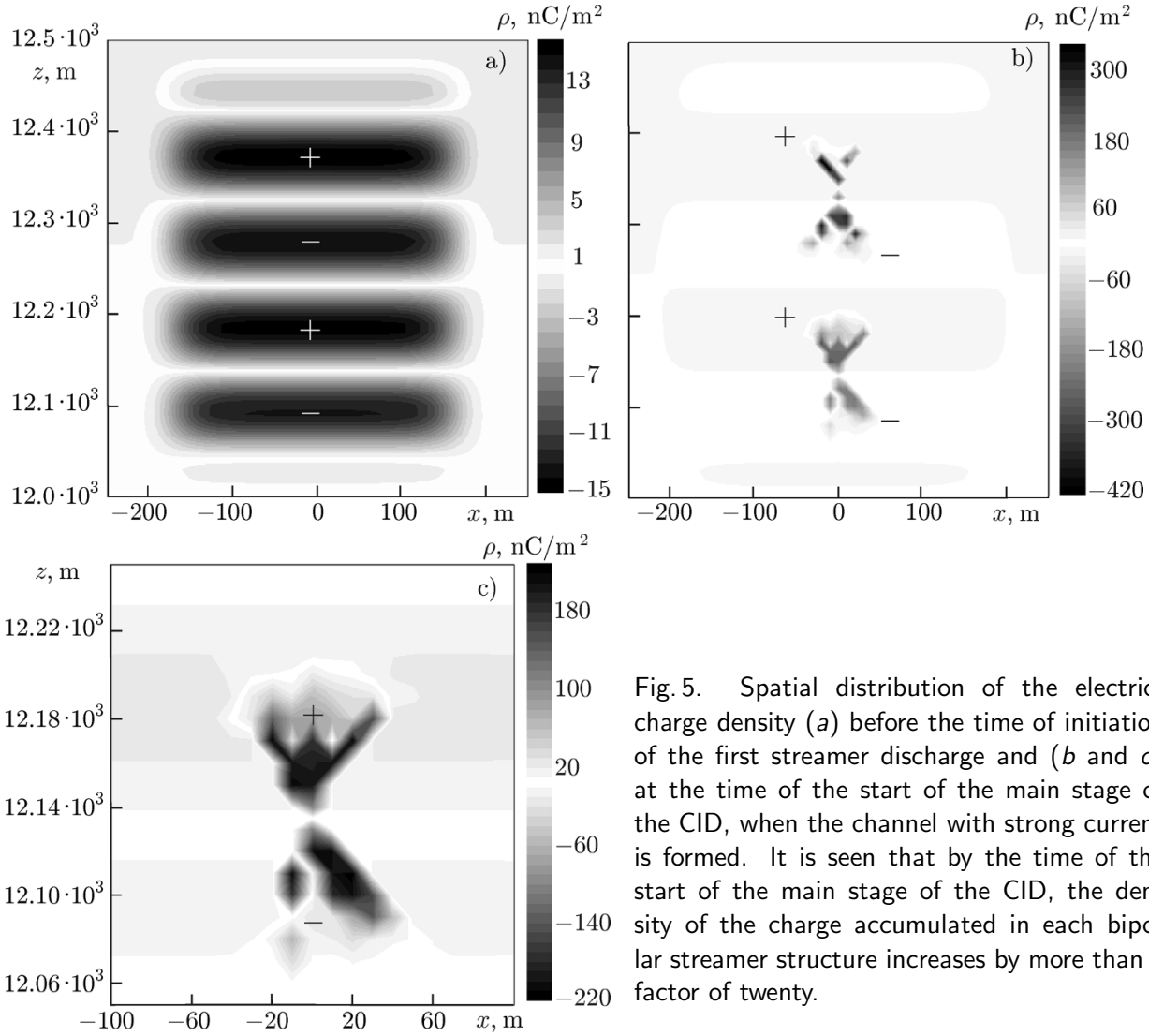

Fig. 5. Spatial distribution of the electric-charge density (*a*) before the time of initiation of the first streamer discharge and (*b* and *c*) at the time of the start of the main stage of the CID, when the channel with strong current is formed. It is seen that by the time of the start of the main stage of the CID, the density of the charge accumulated in each bipolar streamer structure increases by more than a factor of twenty.

current is about 45 kA for a duration of about 10μs, which agrees well with the estimates of the CID current pulse parameters, which were obtained within the framework of the transmission-line approximation [27]. Within the proposed description, it is possible to allow in a natural way for a number of the discharge-current features which cannot be analyzed in the transmission-line approximation. In particular, in this model, it is possible to allow for the deviation of the channel shape from the straight line, the possible branching of the current channel, differences of the current-pulse propagation velocity in different directions, its spatiotemporal asymmetry, etc. These issues, along with checking the assumption of a low level of electromagnetic radiation at the preliminary stage of the CID and formation of a high-power short burst of HF/VHF radiation, will be discussed in the second part of the work. To conclude, we note that the results obtained within the framework of the proposed approach, in particular, the shape and characteristics of the bipolar streamer structure at the preliminary stage of the CID, are in many respects determined by the chosen parameter of the model elements, namely, the size and effective capacitance of an elementary cell, rate of formation of the conducting channel between the cells, and the dependence of its conductivity on the current flowing in it. As was mentioned above, the complexity and the difference in scale of the processes during electric discharges in the thundercloud lead necessarily to their parametrization. However, many questions in gas-discharge physics do not have unambiguous answers; thus, the choice of such parametrization in this model is based on common assumptions on the structure and characteristics of a discharge. It is obvious that the construction of a more exact and justified parametrization requires further experimental and theoretical

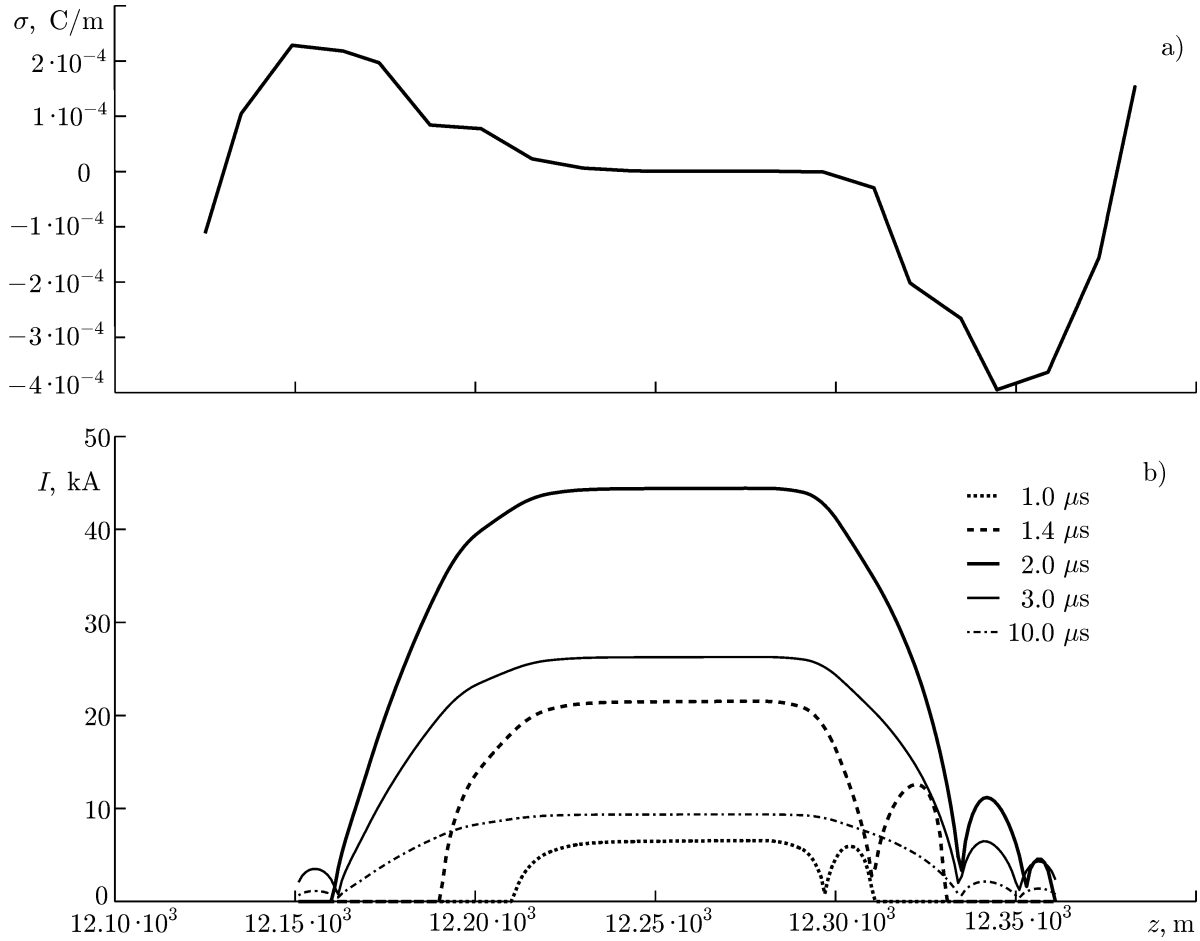

Fig. 6. Distributions of the linear density σ of the electric charge along the conducting channel, connecting the bipolar streamer structures, at the time of its occurrence (*a*) and electric current I in this channel at different moments of time after the start of the main stage of the CID (*b*). The distribution of current along the conducting channel was obtained for the model-time step equal to $\tau = 0.2$ μs.

studies, primarily, in microphysics of discharges in thunderclouds. At the same time, the approach proposed in this paper can also be used for determining the parameter range of the model elements, in which the model describes satisfactorily the observed features of compact intracloud discharges.

4. CONCLUSIONS

We have proposed a new model of a compact intracloud discharge, which suggests that the latter is the result of interaction of two (or more) bipolar streamer structures that form in a strong large-scale electric field. The model assumes that the CID develops in two stages. At the preliminary stage, two or more bipolar streamer structures occur successively in the field of a strong electric field (for example, at the boundary of the main positive and the main negative layers of the space charge or at the boundary of the main positive and negative screening layers). Presumably, the spatiotemporal synchronization of streamer structures is provided by the altitude modulation of the electric field, and the stream instability is a possible source of this modulation. It is shown that during its development, a single bipolar streamer structure accumulates a significant electric charge and is actually a distributed dynamic dipole. The start of the main stage of the CID corresponds to the moment of an electric coupling between the streamer structures, in which the electric charge accumulated at the adjacent ends of the discharges is neutralized over a time much shorter than the duration of the preliminary stage of the CID. In this case, the parameters of the generated

current pulse agrees well with the CID current estimates obtained in the transmission-line approximation. Within the proposed approach, it seems possible to explain a number of observed features of the CID, in particular, the weak radiation (lower than the detection thresholds established in the experiments) at the preliminary stage of a discharge, the formation of a high-power short bipolar pulse of the electric field, and synchronization of the radiation bursts in the VLF/LF and HF/VHF ranges. The radiation of a compact intracloud discharge in different frequency ranges will be considered in the second part of the work.

The authors are grateful to V. A. Rakov for fruitful discussion of the results and important comments, as well as to N. A. Bogatov, A. Yu. Kostinsky, and E. A. Mareev for useful discussions. This work was supported by the Russian Foundation for Basic Research (project Nos. 13–05–01100 and 15–01–06612) and the Ministry of Education and Science of the Russian Federation (State contract No. 14.B25.31.0023).

REFERENCES

1. D. M. Le Vine, *J. Geophys. Res.*, **85**, No. C7, 4091 (1980).
2. J. C. Willett, J. C. Bailey, and E. P. Krider, *J. Geophys. Res.*, **94**, No. D13, 16255 (1989).
3. P. J. Medelius, E. M. Thomson, and E. M. Pierce, in: *Proc. Int. Aerospace and Ground Conf. Lightning and Static Electr., NASA Conf. Publ., 1991*, Vol. 3106, p. 12-1.
4. D. N. Holden, C. P. Munson, and J. C. Devenport, *Geophys. Res. Lett.*, **22**, No. 8, 889 (1995).
5. R. S. Massey and D. N. Holden, *Radio Sci.*, **30**, No. 5, 1645 (1995).
6. R. S. Massey, D. N. Holden, and X. M. Shao, *Radio Sci.*, **33**, No. 3, 1755 (1998).
7. D. A. Smith and D. N. Holden, *Radio Sci.*, **31**, No. 3, 553 (1996).
8. D. A. Smith, X. M. Shao, D. N. Holden, et al., *J. Geophys. Res.*, **104**, No. D4, 4189 (1998).
9. D. A. Smith, R. S. Massey, K. C. Wiens, et al., in: H. Christian, ed., *Proc. 11th Int. Conf. Atmos. Electr., NASA Conf. Publ., 1999*, CP-1999-209261, p. 6.
10. W. Rison, R. J. Thomas, P. R. Krehbiel, et al., *Geophys. Res. Lett.*, **26**, No. 23, 3573 (1999).
11. R. J. Thomas, P. N. Krehbiel, W. Rison, et al., *Geophys. Res. Lett.*, **28**, No. 1, 143 (2001).
12. A. R. Jacobson, S. O. Knox, R. Franz, and D. C. Enemark, *Radio Sci.*, **34**, No. 2, 337 (1999).
13. A. R. Jacobson, K. L. Cummins, M. Carter, et al., *J. Geophys. Res.*, **105**, No. D12, 15653 (2000).
14. D. A. Smith, D. A. Eack, J. Harlin, et al., *J. Geophys. Res.*, **107**, No. D13, 4183 (2002).
15. K. L. Cummins, M. J. Murphy, E. A.. Bardo, et al., *J. Geophys. Res.*, **103**, No. D8, 9035 (1998).
16. A. R. Jacobson and T. E. L. Light, *J. Geophys. Res.*, **108**, No. D9, 4266 (2003).
17. D. A. Smith, M. J. Heavner, A. R. Jacobson, et al., *Radio Sci.*, **39**, No. 1, RS1010 (2004).
18. A. R. Jacobson, *J. Geophys. Res.*, **108**, No. D24, 4778 (2003).
19. T. E. L. Light and A. R. Jacobson, *J. Geophys. Res.*, **107**, No. D24, 4756 (2002).
20. A. R. Jacobson and T. E .L. Light, *Ann. Geophys.*, **30**, No. 2, 389 (2012).
21. A. R. Jacobson, R. H. Holzworth, and X.-M. Shao, *Ann. Geophys.*, **29**, 1587 (2011).
22. K. B. Eack, *Geophys. Res. Lett.*, **31**, No. 20, L20102 (2004).
23. K. C. Wiens, T. Hamlin, J. Harlin, and D. M. Suszcynsky, *J. Geophys. Res.*, **113**, D05201 (2008).
24. A. R. Jacobson and M. J. Heavner, *Mon. Weather Rev.*, **133**, No. 5, 1144 (2005).
25. S. R. Sharma, M. Fernando, and V. Cooray, *J. Atmos. Sol. Terr. Phys.*, **70**, 1251 (2008).
26. F. Lu, B. Zhu, H. Zhou, et al., *J. Geophys. Res. Atmos.*, **118**, 4458 (2013).

27. A. Nag, V. A. Rakov, D. Tsalikis, and J. A. Cramer, *J. Geophys. Res.*, **115**, D14115 (2010).
28. S. Karunarathe, T. C. Marshall, M. Stolzenburg, and N. Karunarathna, in: *Proc. 15th Int. Conf. Atmos. Electr., Norman, Oklahoma, USA, 2014*, P-02-05.
29. T. Wu, W. Dong, Y. Zhang, and T. Wang, *J. Geophys. Res.*, **116**, D03111 (2011).
30. R. Thottappillil, V. A. Rakov, and M. A. Uman, *J. Geophys. Res.*, **95**, No. D11, 18631 (1990).
31. V. A. Rakov, R. Thottappillil, and M. A. Uman, *J. Geophys. Res.*, **97**, No. D9, 9935 (1992).
32. B. Zhu, H. Zhou, R. Thottappillil, and V. A. Rakov, *J. Geophys. Res. Atmos.*, **119**, No. 6, 2699 (2014).
33. A. V. Gurevich, G. M. Milikh, and R. Roussel-Dupre, *Phys. Lett. A*, **165**, 463 (1992).
34. A. V. Gurevich and K. P. Zybin, *Phys. Usp.*, **44**, No. 11, 1119 (2001).
35. A. A. Gurevich, K. P. Zybin, and R. A. Roussel-Dupre, *Phys. Lett. A*, **254**, 79 (1999).
36. V. Cooray, G. Cooray, T. Marshall, et al., *Atmos. Res.*, **149**, 346 (2014).
37. S. Arabshahi, J. R. Dwyer, A. Nag, et al., *J. Geophys. Res. Space Phys.*, **119**, 479 (2014).
38. G. T. Zatsepin and V. A. Kuz'min, *JETP Lett.*, **4**, No. 3, 76 (1966).
39. A. Nag and V. A. Rakov, *J. Geophys. Res.*, **115**, D20102 (2010).
40. H. E. Tierney, R. A. Roussel-Dupre, E. M. D. Symbalisty, and W. H. Beasley, *J. Geophys. Res.*, **110**, D12109 (2005).
41. R. A. Roussel-Dupre and A. V. Gurevich, *J. Geophys. Res.*, **101**, No. A2, 2297 (1996).
42. J. R. Dwyer and L. P. Babich, *J. Geophys. Res.*, **116**, A09301 (2011).
43. C. L. Silva and V. P. Pasko, *J. Geophys. Res. Atmos.*, **120**, No. 10, 4989 (2015).
44. L. Niemeyer, L. Pietronero, and H. J. Wiesmann, *Phys. Rev. Lett.*, **52**, No. 12, 1033 (1984).
45. E. R. Mansell, D. R. MacGorman, C. L. Ziegler, and J. M. Straka, *J. Geophys. Res.*, **107**, No. D9 (2002).
46. D. I. Iudin, V. Yu. Trakhtengertz, and M. Hayakawa, *Phys. Rev. E*, **68**, No. 1, 016601 (2003).
47. P. R. Krehbiel, J. A. Riousset, V. P. Pasko, et al., *Nature Geosci.*, **1**, 233 (2008).
48. H. J. Wiesmann and H. R. Zeller, *J. Appl. Phys.*, **60**, No. 5, 1770 (1986).
49. N. Femia, L. Niemeyer, and V. Tucci, *J. Phys. D: Appl. Phys.*, **26**, No. 4, 619 (1993).
50. M. Hayakawa, D. I. Iudin, and V. Yu. Trakhtengerts, *J. Atmos. Sol. Terr. Phys.*, **70**, No. 13, 1660 (2008).
51. J. A. Riousset, V. P. Pasko, P. R. Krehbiel, et al., *J. Geophys. Res.*, **112**, D15203 (2007).
52. D. I. Iudin, F. D. Iudin, and M. Haykawa, *Radiophys. Quantum Electron.*, **58**, No 3, 173 (2015).
53. E. R. Mansell, D. R. MacGorman, C. L. Ziegler, and J. M. Straka, *J. Geophys. Res.*, **110**, D12101 (2015).
54. V. Yu. Trakhtengerts, *Dokl. Akad. Nauk SSSR*, **308**, No. 3, 584 (1989).
55. E. A. Mareev, A. E. Sorokin, and V. Yu. Trakhtengerts, *Plasma Phys. Rev.*, **25**, No. 3, 261 (1999).
56. Yu. P. Raizer, *Gas Discharge Physics*, Springer, Berlin (1997).
57. U. Ebert and D. D. Sentman, *J. Phys. D: Appl. Phys.*, **41**, No. 23, 230301 (2008).
58. M. G. Andreev, N. A. Bogatov, A. Yu. Kostinskiy, et al., in: *Proc. 15th Int. Conf. Atmos. Electr., Norman, Oklahoma, USA, 2014*, O-03-98.
59. A. Yu. Marshall and W. D. Rust, *J. Geophys. Res.*, **96**, No. D12, 22297 (1991).
60. M. Stolzenburg, T. C. Marshall, and P. R. Krehbiel, *J. Geophys. Res.*, **2010**, 115, D19202 (2010).
61. J. A. Riousset, V. P. Pasko, P. R. Krehbiel, et al., *J. Geophys. Res.*, **115**, A00E10 (2010).

62. S. S. Davydenko, T. C. Marshall, and M. Stolzenburg, in: *Proc. XIV Int. Conf. Atmos. Electr.*, Rio de Janeiro, Brazil (2011), p. 230.

63. I. Gallimberti, G. Bacchiega, A. Bondiou-Glergerie, and P. Lalande, *C. R. Phys.*, **3**, No. 10, 1335 (2002).

64. S. S. Davydenko, D. I. Iudin, V. Yu. Klimashov, et al., in: *Proc. 15th Int. Conf. Atmos. Electr., Norman, Oklahoma, USA, 2014*, P-08-19.